Journal of Hydrology 424–425 (2012) 184–195

Contents lists available at SciVerse ScienceDirect

Journal of Hydrology

journal homepage: www.elsevier.com/locate/jhydrol

Magnetic resonance sounding and radiomagnetotelluric measurements used to characterize a limestone aquifer in Gotland, Sweden

Nils Perttu [a,*], Lena Persson [b], Mikael Erlström [b], Sten-Åke Elming [a]

[a] Division of Ore Geology and Applied Geophysics, Luleå University of Technology, SE-971 87 Luleå, Sweden
[b] Geological Survey of Sweden, PO Box 670, SE-751 28 Uppsala, Sweden

ARTICLE INFO

Article history:
Received 21 March 2011
Received in revised form 14 November 2011
Accepted 29 December 2011
Available online 8 January 2012
This manuscript was handled by Philippe Baveye, Editor-in-Chief

Keywords:
Groundwater
Gotland
Magnetic resonance sounding
Radiomagnetotelluric
Karst aquifer
Geophysical methods

SUMMARY

Almost all drinking water in Gotland is groundwater and is mainly found in karst limestone. However, the unpredictable location and geometry of the karst cracks and caverns makes it very difficult to estimate groundwater storage and movement, as well as contaminant transport. The aim of this study was to test the performance of different geophysical techniques like Magnetic Resonance Sounding (MRS), Radiomagnetotelluric (RMT), Vertical Electrical Sounding (VES) and Ground Penetrating Radar (GPR) to characterize aquifers in Gotland, in respect to geometry and storage as well as connectivity over a wider area. The investigated area is located on the south-eastern part of Gotland. The geology here is dominated by 50–60 m thick successions of limestone that gradually turn into marlstone. The use of multiple techniques has shown to give a more coherent interpretation. However, the shallow penetration depth of GPR and the lack of soil cover in some places of the investigated area limit the use of geoelectrical methods and GPR. With MRS, water are found down to 60 m in depth, with a maximum water content at depths of 20–30 m. This coincides with the most resistive sections of the limestone. The water content varies between 0% and 3%, with a relaxation time (T_{1MRS}) less than 400 ms suggesting that the aquifer is hosted in small fractures, molds and vugs rather than larger karst fractures and caverns. Two potential aquifers were identified with MRS, possibly separated by marlstone. From modeling it can be seen that such boundary separating two aquifer apart can be more easily discriminated in the N/S-, than in the E/W direction. In summary, MRS is therefore the only method in this survey that can detect and determine the vertical and lateral distribution of water within the aquifer together with the total volume of free water.

The RMT method has shown to be effective in characterizing the limestone/marl interface, but also to locate anomalous low resistive zones, possibly associated with salt water. RMT also helps to constrain the final MRS model by choosing a suitable regularization for the MRS 3D inversion. All together, the combination of MRS and RMT seems most efficient of the tested methods and therefore most promising for future groundwater explorations in geological environments like in eastern Gotland.

1. Introduction

Almost all drinking water in Gotland is groundwater and is mainly found in karst limestone. The unpredictable location and geometry of the karst cracks and caverns makes it very difficult to estimate groundwater storage and movement, as well as contaminant transport (Eklund, 2005; Vattenmyndigheten, 2007). The access to groundwater is usually related to dense limestone lithologies. Relatively good aquifers are found in the mid-northern part of Gotland, whereas the groundwater access is limited in the northern part, the south-western coast and the eastern part of Gotland (Fig. 1; key map). Since most groundwater is formed during a period stretching from November to April, a shortage of drinking water can also occur locally during the summer months. The thin and in some areas lack of soil cover makes the aquifers vulnerable to contaminants originating from pesticides and fertilizers used in agriculture. When examining the water quality from official water supplies in Gotland, 25% of the water supplies had residues of pesticides (Vattenmyndigheten, 2007). Also, well records stored at the Geological Survey of Sweden (SGU) showed that from 149 investigated wells as much as 61% of the wells had a raised chloride content defined here as >50 mg/l and 26% exceeded the taste limit of 300 mg/l (Olofsson, 1996; SEPA, 2007). The salt affected wells were not only located along the coastline but wells with concentrations up to a couple of 1000 mg/l can be found as far as 20–30 km inland, suggesting that the saline water not only originates from sea water intrusion but are also fossil (Eklund, 2005; Lindewald, 1985). The dependence of groundwater and the complexity and vulnerability of aquifers in Gotland demands for

* Corresponding author. Tel.: +46 920 491884; fax: +46 920 491199.
E-mail addresses: nilper@ltu.se, Nils.Perttu@ltu.se (N. Perttu).

0022-1694/$ - see front matter © 2012 Elsevier B.V. All rights reserved.
doi:10.1016/j.jhydrol.2011.12.042

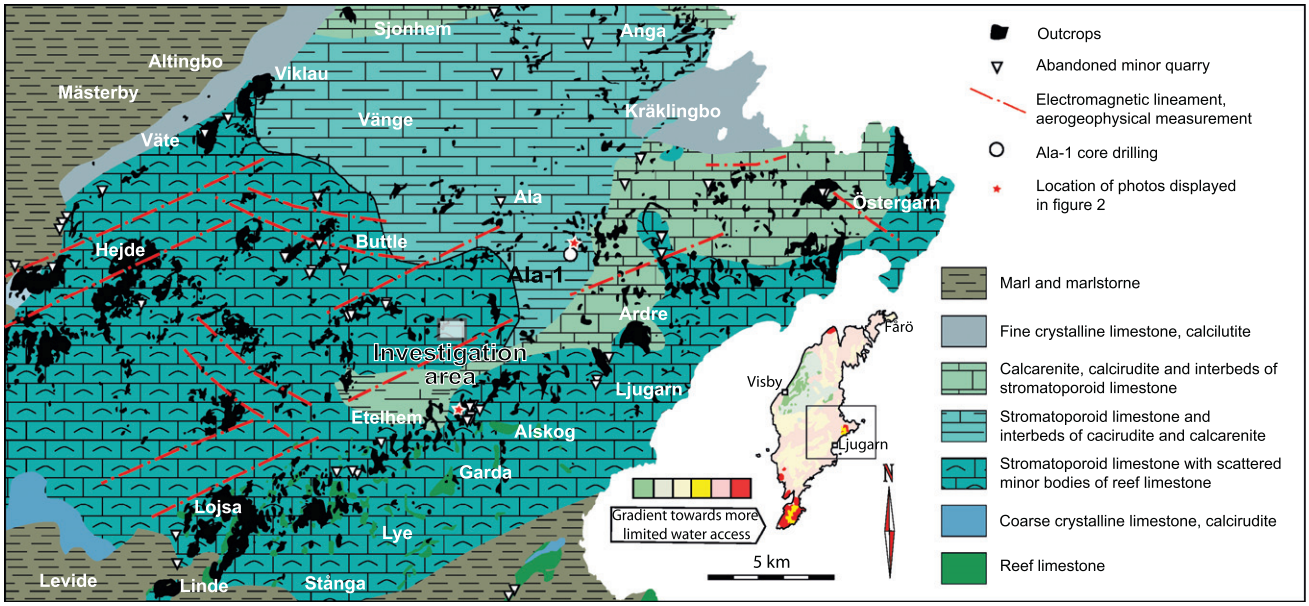

Fig. 1. Key map showing the groundwater distribution of Gotland together with a bedrock map of the central eastern part of Gotland. The investigation area is marked with a transparent rectangle.

an efficient tool to characterize groundwater supplies regarding their geometry, storage and hydraulic properties as well as connectivity over a wider area.

The aim of this study is to test the performance of different geophysical techniques like Magnetic Resonance Sounding (MRS), Radiomagnetotelluric (RMT), Vertical Electrical Sounding (VES), and Ground Penetrating Radar (GPR) to characterize an aquifer in Gotland. Furthermore, we want to evaluate how and when these different methods can be used together most efficiently. Drilling is the most capable and accurate method to detect aquifers, however the unpredictable occurrence of water in karst over larger areas makes the drilling cost substantial. The petrophysical properties of karst aquifers are to a large extent influenced by the water content and salinity, e.g. electrical conductivity determined from VES and RMT measurements (Guerin and Benderitter, 1995; Linde and Pedersen, 2004) and the dielectric constant from GPR measurements (Al-fares et al., 2002; Anchuela et al., 2009). MRS, in contrast to other geophysical techniques, gives a direct measure of the free water content, but also the pore size distribution with depth (Legchenko and Valla, 2002). With MRS it is possible to determine both storage and hydraulic related parameters far less ambiguous than with classical geophysical technique (Lubczynski and Roy, 2003). MRS has also proven to be successful method in detection and characterization of karst aquifers using 1D or 2D inversion (Boucher et al., 2006; Girard et al., 2007; Legchenko et al., 2008; Vouillamoz et al., 2003). However, karst aquifers are usually 3D structures. This study illustrates a working methodology for 3D investigation and demonstrates the possibilities and limitations of using MRS for groundwater exploration in a geological environment such as in Gotland.

2. Geological setting

Three major areas on Gotland are dominated by dense limestone lithologies. One area is trending northeast from Visby to Fårö, a second area covers large parts of central Gotland and the third area is found in the southernmost part (Fig. 1; key map). These areas coincide with topographic highs, thin Quaternary cover and frequent karstification. Reefs, talus deposits (calcirudite) and lagoonal carbonates are frequent. Between these limestone dominated areas there are low lying areas dominated by marl and marlstone with frequent intercalations of limestone (calcarenite and calcilutite). The Quaternary cover is here thicker and the bedrock is mainly exposed in quarries, temporary trenches and ditches.

The limestone lithologies in the central parts of Gotland (Fig. 1) are up to 20–60 m thick and are dominated by stromatoporoid reefal limestone, biocalcarenite and ruditic limestone (Erlström et al., 2009). The deposition occurred in shallow water reef associations in laterally varying conditions. Much of the exposed bedrock in the area around Ala-Ardre is composed of 10–40 cm thick nodular beds of stromatoporoid limestone interbedded by 5–10 cm thick beds of biocalcarenite. Layers with conglomeratic and very coarse limestone with chaotic bedding occur frequently (Fig. 2a). These reflect a proximal deposition close to the reef front and they are likely formed as debris flows adjacent to the reef bodies. The bedrock is frequently exposed or only covered by a thin soil cover. The exposed bedrock surface is also frequently affected by karstification which has resulted in up to 1 m deep karren structures (Fig 2b).

There are unfortunately very few observations on the subsurface lithological succession in the eastern part of central Gotland. One core drilling at Ala (Ala-1; Fig. 1) is the only data set that gives a detailed picture of the subsurface bedrock succession. The borehole data give a maximum limestone thickness in the range of 50–60 m. The limestone sequence is dense and well indurated and overlies beds of dark gray marl and marlstone. The bedding is irregular and part of the interval has a reef like structure giving a chaotic bedding structure of the rock. Fractures occur relatively frequently and are commonly subvertical and undulating with a varying open aperture. Calcite infillings and complete sealing of the original fractures are common. The boundary towards the underlying marl/marlstone is gradual. The bedding becomes more regular and the amount of marlstone interbeds increase with depth. There is also a higher frequency of fractures occurring along the bedding planes indicating planes of weakness parallel to the bedding.

Beside limestone there occur scattered thin beds and layers of marl in the sequence.

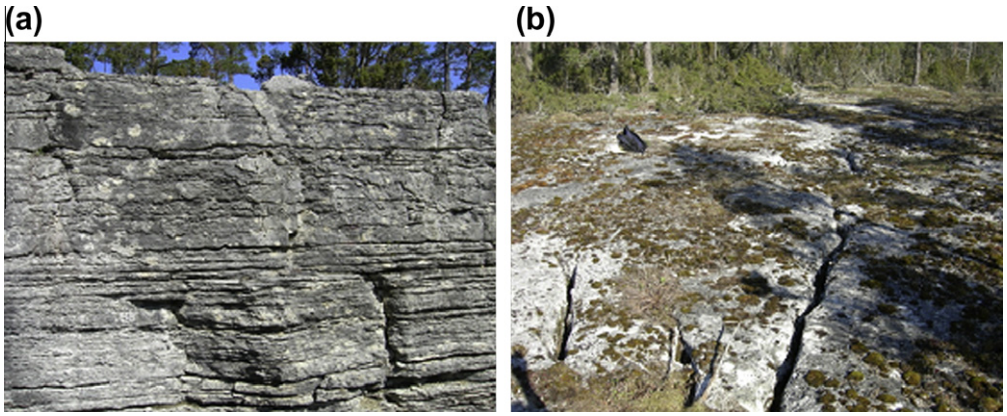

Fig. 2. (a). Typical bedding in a limestone outcrop in the Ala-Ardre area. The limestone is composed of coarse calcirudite and stromatoporoid limestone, often with a proximal origin to a reef. (b) Bedrock surface close to the Ala borehole. Note the typical karren structures in the topmost part of the limestone.

The limestone is in general very dense and the porosity is generally very low (<5%). This is caused by diagenetic alteration of the limestone with recrystallization and a high amount of secondary calcite mineralizations filling most of the original pore space. The observed porosity is related to fractures and molds and vugs. The effective porosity is therefore generally lower than the total because of the isolated pores.

As a whole the limestone sequence can be characterized as a fractured reservoir with only a few percent reservoir capacity of the total volume. Smaller faults, fracture zones and lineament occur frequently with major trends corresponding to 270–310°E and 40–60°E. The water well drilling in the area have shown local water inflow in the limestone unit (between 0 and 1500 l/h), however the main inflow of water occur in the interface between the underlying marl and the basal limestone layers. Here a capacity of 5000–6000 l/h has been measured.

2.1. Investigated area

The investigated area is located on the south-eastern part of Gotland, about 10 km north-west of the village of Ljugarn (Fig. 1). Measurements have been made along a small road in a partly clear cut area within the pine forest (Fig. 3). The soil cover is thin and outcrops of limestone can be found in the north-western as well as the south-eastern part of the study area. The area is quite flat with a mean elevation of about 50 m above sea-level.

3. Method and result

For this study, the Complex Resistivity (CR) method have been used to determine the resistivity of borehole samples from Ala-1 in the geophysical laboratory at Luleå University of Technology (LTU) and four different geophysical techniques have been used in field (listed in Table 1): Radiomagnetotelluric (RMT); Vertical Electrical Sounding (VES); Ground Penetrating Radar (GPR) and Magnetic Resonance Sounding (MRS). The MRS, VES and GPR measurements were carried out during two weeks in August, 2009, whereas the RMT data were gathered in the beginning of November 2009.

3.1. Complex Resistivity (CR)

3.1.1. Method and field setup

The Complex Resistivity (CR)/Spectral Induced Polarization (SIP) instrument used in this study has been developed at the petrophysical laboratory in Luleå University of Technology and measures the resistivity and phase for frequencies varying between 0.1 and 30 Hz against a reference resistance that can be varied between 2, 10, 100 and 1000 kΩ for both cylindrical and cubic rock samples. The data has then been fitted to the Cole–Cole model (Pelton et al., 1978):

$$\rho(\omega) = \rho_0\left\{1 - m\left(1 - \frac{1}{1 + (i\omega\tau)^c}\right)\right\} \quad (1)$$

using a Monte Carlo inversion scheme in MathCAD developed by Hans Thunehed (Triumf et al., 2000), where ρ is the resistivity at the frequency ω, ρ_0 is the dc resistivity and m, τ and c are the chargeability, time constant and shape factor, respectively. CR/IP parameters have shown to be related to the clay content and permeability of rocks (Börner, 1996; Worthington and Collar, 1982).

3.1.2. Result

CR measurements were made on eight saturated samples at depths of 8, 28, 56 and 70 m from the Ala-1 borehole. The limestone is rather homogenous at depths between 8 and 28 m (5000–14,000 Ωm) but between 56 and 70 m the interbedding of marl becomes more frequent (140 and 2200 Ωm) and the resistivity decreases accordingly. An example of one CR measurement is shown (Fig. 4a) from 70.1 to 70.3 m depth. The porosity has been estimated for each sample by weighting the sample wet, dry and immersed in water. Higher porosities (3–5%) are here normally associated with higher visible content of marl, whereas lower porosities (0.8–1%) are associated with more massive limestone. There is an exponential correlation between porosity and resistivity (Fig. 4b), however between other parameters no correlations were found.

3.2. Radiomagnetotelluric (RMT)

3.2.1. Method and field setup

The Radiomagnetotelluric (RMT) method makes use of the signal in the frequency range between 15 and 250 kHz from long-distance radio transmitters. Induction of currents in the ground generates electric and magnetic fields and with the tensor RMT technique, two horizontal components of the electric field and three components of the magnetic field are measured simultaneously. The ratio between the horizontal electric and magnetic field components for each frequency are directly related to the resistivity of the ground. The signal at lower frequencies penetrates deeper into the ground and the variation of resistivity with depth can then be determined. The RMT data were acquired with the EnviroMT system, developed at Uppsala University (Bastani, 2001).

The RMT method has earlier been used for groundwater studies in karst environments; e.g. Turberg et al. (1994) used the scalar

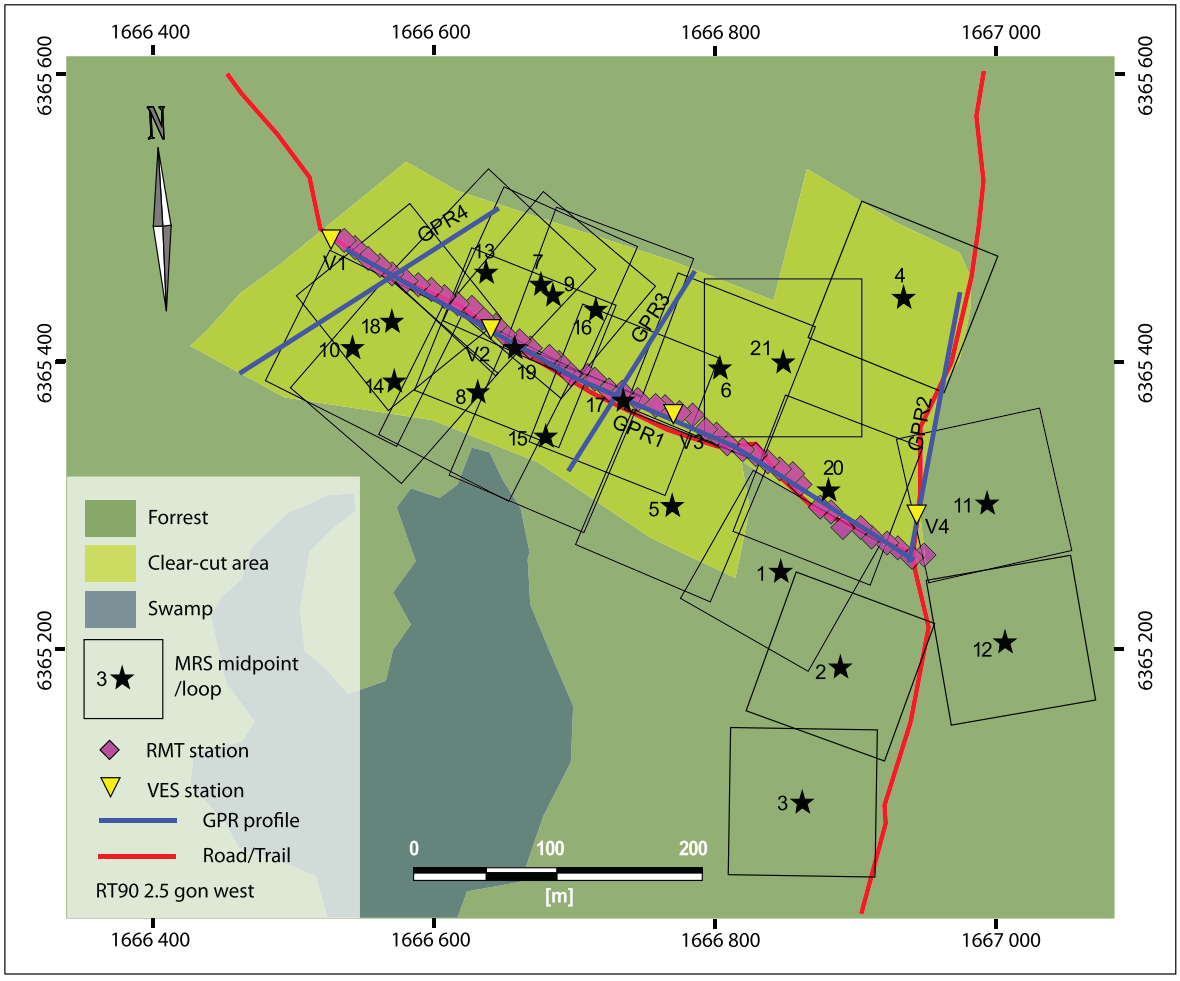

Fig. 3. Investigation area located about 10 km north-west of the village of Ljugarn. The layout and centers of the MRS loops are numbered and shown by squares and stars, respectively. The blue lines denote GPR profiles and the RMT and VES stations are marked by the purple and yellow symbols, respectively. (For interpretation of the references to colour in this figure legend, the reader is referred to the web version of this article.)

Table 1
Methods, instruments and inversion software used in the study.

Method	Instrument	Manufacture	Interpretation software	Manufacture
MRS	Numis-Plus	Iris Instruments	Samovar	Anatoly Legchenko[a]
RMT	EnviroMT	Uppsala University	Rebocc (modified)	Thomas Kalscheuer[b]
VES	SAS4000	ABEM	IPI2win	Moscow State University
GPR	RAMAC	Malå Geoscience	Reflex2Dquick	Sandmeier scientific software
CR	ComplexRes	LTU	Mathcad-sheet	Hans Thunehed[c]

[a] LTHE, Grenoble, France.
[b] ETH Zürich, Switserland.
[c] Geovista AB, Luleå, Sweden.

form of the RMT method for hydrogeological applications. More recent examples from RMT groundwater exploration in glacial and sandy formations can be found in Pedersen et al. (2005) and Ismail et al. (2011). Linde and Pedersen (2004) showed evidence of electric anisotropy in limestone on the island of Gotland and the RMT method also showed to be successful in delineating the stratigraphy of sedimentary layers of limestone and marl (Erlström et al., 2009; Persson et al., 2008).

The total length of the measured RMT profile in the present study was 450 m and all measurements were made along a small road with a sampling distance of 10 m and 50 stacking. Overall the data quality was good with a S/N larger than 10 dB from 32 to 40 transmitters for each station. The measured electric and magnetic fields were then transformed into resistivity and phase at each frequency and station. After processing of the RMT data, with a band averaging technique (Bastani, 2001), eight frequencies from 14 to 226 kHz were used for the 2D-inversion.

For the modeling of the RMT data we used the modified version of the inverse code Rebocc, which allows for displacement currents (Kalscheuer et al., 2008; Siripunvaraporn and Egbert, 2000). REBOCC stands for REduced Basis OCCam's Inversion and the inversion method used is of Occam type and is based on smoothing through regularization. The determinant data were used in the 2D-inversion. The theoretical 2D determinant data can be considered as the arithmetic mean of the transverse electric (TE) and magnetic (TM) mode and is preferable to use when the regional strike is unknown or when 3D-structures are present. In these cases the determinant data may show reliable models compared to the joint TE and TM mode (Pedersen and Engels, 2005).

3.2.2. Result

The observed apparent resistivity varies between ca. 300 and 1400 Ωm (Fig. 5a). In the middle of the profile a low resistive structure is present. For the lowest frequencies the resistivity decreases

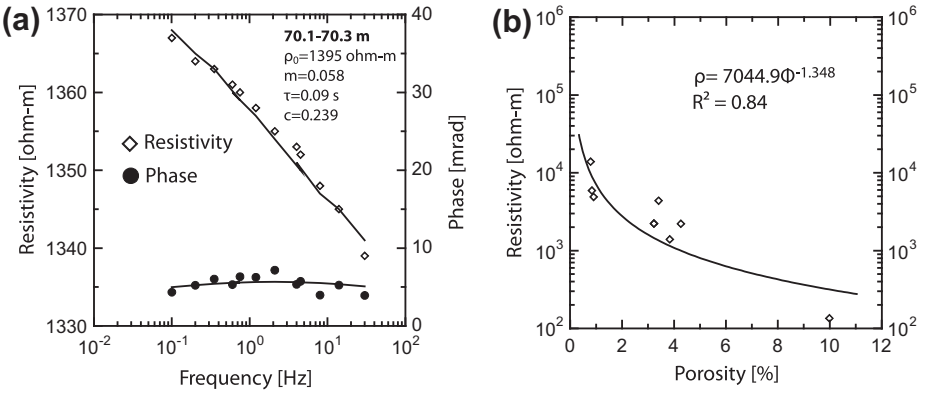

Fig. 4. (a) Inversion fit (solid line) to measured resistivity (diamonds) and phase (circles). (b) Resistivity (ρ) and Porosity (Φ) correlation for rock samples at depths between 8 and 72 m. The increase of marl is shown in the increase in Φ.

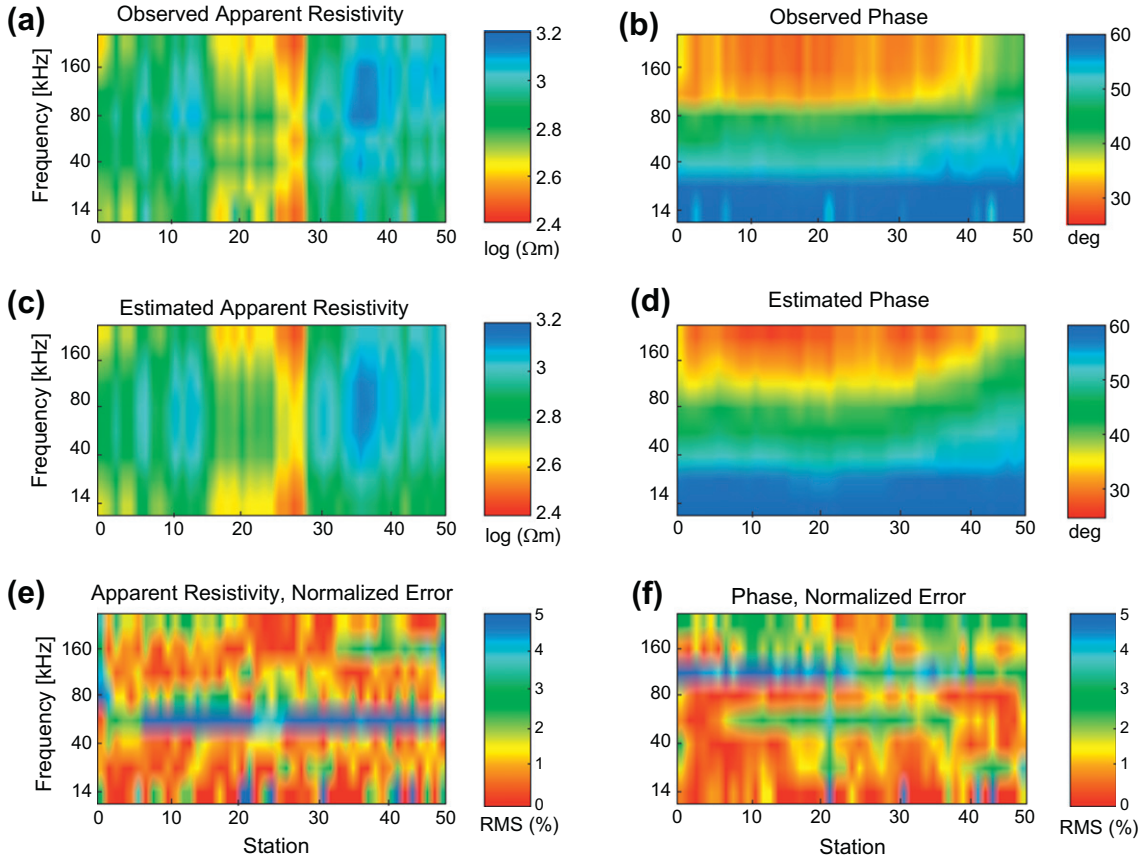

Fig. 5. The inversion fit of RMT data showing a) observed (a) apparent resistivity and (b) phase; calculated (c) apparent resistivity and (d) phase together with the and normalized error (%) for (e) apparent resistivity and (f) phase.

slightly and moreover the phase increases to >50° (Fig. 5b) indicating a conductor at larger depths. The corresponding model response from the 2D-inverson (Fig. 5c and d) with an error floor of 3% on the apparent resistivity, shows a normalized RMS of 2.3% (Fig. 5e and f), reached after seven iterations.

The resistivity model from the 2D-inversion (Fig. 12a), shows principally three layers; at the top, a thin low resistive layer (<300 Ωm), that probably correspond to the overburden followed by a more resistive layer (>1000 Ωm) indicating massive limestone. The third layer is characterized by a lower resistivity (<300 Ωm) indicating marl. The thickness of the high resistive limestone layer varies significantly along the profile, from 20 up to 60 m. The low resistivity section found in the limestone layer in the middle of the profile (150–250 m) may be caused by a higher content of marl or fractured (faulted) limestone filled with conductive material. A highly conductive part (<30 Ωm) is also found here, below 80 m in depth. This anomalous conductive zone may indicate the presence of saline groundwater. The resolution of the RMT method is however rather limited at this depth and no detailed model of its distribution can be obtained.

3.3. Vertical Electrical Sounding (VES)

3.3.1. Method and field setup

Four VES measurements were conducted along the RMT profile with a distance of ca. 100 m apart. The Schlumberger configuration

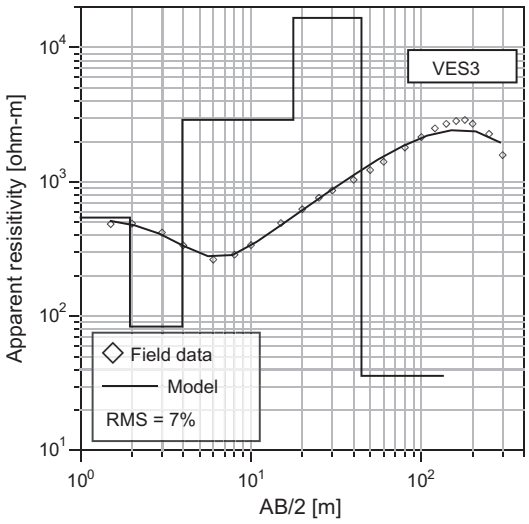

Fig. 6. An example of a Vertical Electrical Sounding (VES3) illustrating the inversion fit and the model resistivity distribution with depth.

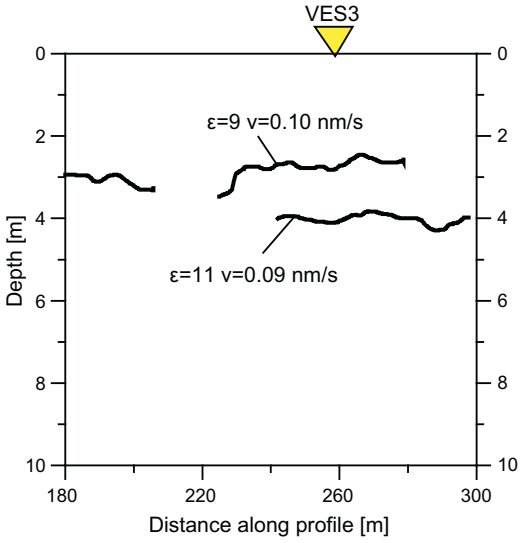

Fig. 7. The GPR section between profile coordinates 180 and 300 m. Two major horizontal reflections are visible at depths of 2.5–3 m as well as at 4 m.

was used with a maximum AB/2 distance of 300 m, and a stacking between 4 and 6, which resulted in an average standard deviation of the apparent resistivity data of less than 0.1%. The investigated area has a thin but sufficient soil cover to inject a current usually between 50 and 100 mA. Depending on the karst being filled with air or water, local high or low resistivity anomalies may be expected. The models have been constrained by RMT/CR data.

3.3.2. Result

The VES data are of quite good quality and models with 4–5 layers can be fitted with a RMS varying from 2% to 7% from site to site. The apparent resistivity varies between 200 and 6000 Ωm. In the western and eastern part of the profile (VES1, VES2 and VES4; Fig. 12a) the soil cover is about 1.5 m. The underlying limestone can be divided into one medium resistive layer (ca. 1000 Ωm) with a thickness of 10–20 m and a second more resistive layer with a thickness of 20–40 m with a resistivity of 10,000–30,000 Ωm, e.g. VES3 (Fig. 6), which is interpreted as massive limestone with low porosity and little or no interference of marl. The apparent resistivity curve shows a steep negative gradient at AB/2 distances larger than 200 m, which is an indication of marlstone, starting at depths of 40–70 m. However the AB/2 distances are too short to determine the true resistivity of this layer. VES3, situated in the middle of the profile show a thicker soil cover (ca. 4 m), where the low resistivity of the second layer could be an indication of higher content of clay or peat (Fig. 6).

3.4. Ground Penetrating Radar (GPR)

3.4.1. Method and field setup

The GPR measurements were conducted with a RAMAC system, using a 250 MHz shielded antenna (Malå Geoscience), with a sampling frequency of 2500 MHz and a trace interval of 10 cm. The number of stacking was set to 8. One profile is located along the road (GPR1) coinciding with the RMT profile whereas the three other profiles (GPR2, GPR3 and GPR4) are trending SW–NE (Fig. 1) perpendicular to GPR1 and crossing it in the southeastern, middle and northwestern part, respectively. The processing of the GPR data included time zero adjustment, subtraction of DC-shift and dewow, gain function, bandpass filter and background removal. A propagation velocity of 0.095 m/ns corresponding to the average velocity of the 4 m thick soil cover was used for the time-depth conversion of the radargram (Fig. 12c). Limestone has a dielectric constant corresponding to 7–8 (Daniels, 2004), which would create clear reflections at the boundary of the water or air filled cracks, as long as the fractures are sufficiently open.

3.4.2. Result

GPR clearly distinguish the soil–limestone interface in the area at a depth of 0.5 (in the western part) to about 4 m (in the middle to the north eastern part). The unsaturated and saturated soil cover shows a good correspondence to VES3 with a velocity of 0.1 and 0.09 nm/s, respectively (Fig. 7). The limestone seems to be homogenous with no obvious reflections from cracks or fissures. The depth of penetration is difficult to evaluate since it is complicated to assess if the radar waves are attenuated or the material of propagation is homogenous. However, below the depth of 10 m, the signals are weak and clearly affected by noise, without any resemblance of reflections.

3.5. Magnetic Resonance Sounding (MRS)

3.5.1. Method and field setup

MRS is a non invasive geophysical technique that energizes the hydrogen nuclei in groundwater by transmitting a resonance electromagnetic pulse with the Larmor frequency. The energized nuclei then generate a secondary magnetic resonance signal, i.e. measured on the surface. The method and principles are thoroughly described in Legchenko and Valla (2002) and Hertrich (2008). The initial amplitude (E_0) of the Free Induction Decay (FID) signal induced in the antenna by the relaxation of the nuclei is directly related to the water content. The decay time of the relaxation (T_2^*) is related to the mean pore size of the material, and hence the grain size and hydraulic conductivity. However, T_2^* is highly influenced by magnetic inhomogeneities, which makes it less reliable in estimating the mean pore size. The longitudinal relaxation (T_{1MRS}) has shown to be more consistent (Legchenko et al., 2004) and can be determined by the saturation recovery technique using a double pulse sequence (Fig. 8a and b), where the relationship between the signal amplitudes and the delay between the pulses returns the T_{1MRS}. By increasing the pulse moment, signals can be retrieved from deeper parts of the subsurface and the vertical distribution of water can be determined. The MRS measurements on Gotland were carried out along roads crossing the investigation area (Fig. 3), using a 100 m square loop. MRS data from 21 sites were interpreted with the inversion software Samovar

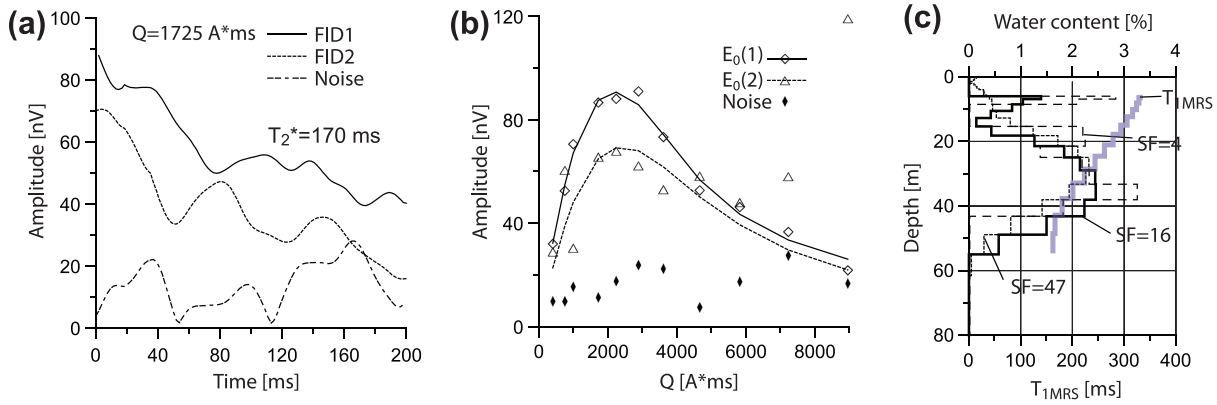

Fig. 8. (a) Filtered signals from the pulse moment (Q) 1725 A ms at site 1, shows a relatively short T_2^*. (b) T_{1MRS} inversion fit of site 1, where diamonds and triangles are data and continues and hatched lines are the model curves of the first and second pulse, respectively. Black dots are measured noise. (c) The inverted models with increasing Smoothing Factors (SF) from site 1, illustrates the water content and T_{1MRS} (thick continuous line) distribution with depth.

v11.3, based on the least square solution with regularization (Legchenko and Valla, 1998), where all solutions within a certain range of smoothing (SF) at the given noise are valid solutions (Fig. 8c). In the investigated area, the magnetic field intensity was about 50,700 nT and the inclination of the field was 71°. Loops have been positioned side by side in the eastern part and half-side overlapped loops in the western part in an attempt to get a continues image of the water content distribution. The different ways of positioning depend on the terrain and the change in signal amplitude from site to site. The signature of karst aquifers is defined from the relaxation time (T_{1MRS}). Karst aquifers have long relaxation times ($T_{1MRS} \rightarrow$ 1000 ms), whereas porous medium have shorter relaxation times ($T_{1MRS} <$ 400 ms) (Legchenko et al., 2008). Relaxation times (T_2^*) lower than 40 ms are not measureable with our Numis-equipment and is usually associated with clay (Shirov et al., 1991) or in this case marl. The porosity of the limestone matrix is usually low (<1%; Boucher et al. (2006)) as can also be seen from the porosity estimates of more homogenous limestone samples from the Ala-1 borehole (Section 3.1.2).

3.5.2. Result of 1D inversion

T_2^* varies between 120 and 250 ms and maximum amplitudes varies between 43 and 93 nV with higher amplitudes along a NW–SE trending section in the central part of the investigation area (Fig. 11a). From 1D inversion, the maximum water content and distribution can vary between equivalent models by more than 1% (Fig. 8c). However, the general trend is that water is found between depths of 0 and 60 m, with maximum water content between different sites varying between 0.9% and 3.5% at depths of 15–40 m, which are within the same range as geological observations in the area (Section 2). The T_{1MRS} inversions are generally of poor quality due to high levels of noise but also due to the second pulse moment have been set smaller than the first pulse, which undoubtedly affects the quality and reliability of the T_{1MRS}-result. The apparent (measured) and inverted T_{1MRS} are still lower than 400 ms (Fig. 8c) in all sites, which suggest that the aquifer medium is not associated with larger cracks, but rather with a more porous rock.

3.5.3. Method of 3D inversion

The 3D inversion builds up a model of cells or voxels over the investigated area. The effect of each saturated cell on the different loops (in this case 21) is computed individually by linear filters. It is therefore important to determine the maximum volume or number of cells exposed by the excitation field of one loop to minimize the computing time of the inversion. The maximum depth of penetration is automatically modeled in Samovar for a 1 m thick layer of

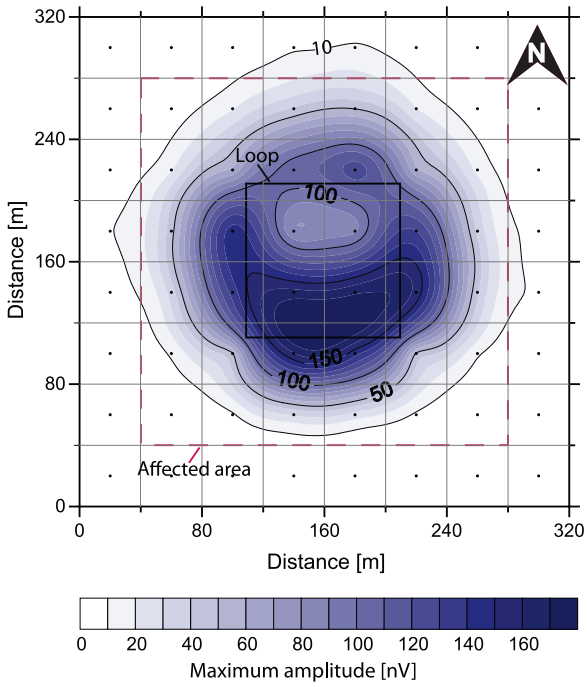

Fig. 9. Modeling of the signal distribution for a 100 m square loop with the geomagnetic field condition and resistivity distribution typical for the area, created by a cell ($40 * 40 * 40$ m^3) with 40% of water situated between 10 and 50 m. The cell is moved over the area with an equidistance of 40 m. The exposed affected area of one loop is defined for the 3D inversion as $240 * 240$ m^2.

100% water, which in the case of a 100 m square loop and with the resistivity distribution determined from RMT, amounts to about 120 m. The area of one cell has been selected to $40 * 40$ m^2 and the affected area of one loop is here modeled for a $320 * 320$ m^2 area, using saturated cells of $40 * 40$ m^2 moved with 40 m equidistance within the area. The aquifer geometry from Site 1 has been used as input model, as it reasonably well corresponds to an average site characteristic of the investigation area. The water content has cautiously been overestimated to 40%, as this could correspond to larger fractures or cavities in natural limestone. The asymmetry of the signal distribution is due to the inclination of the geomagnetic field, which will render higher amplitudes in the southern part of the loop (Fig. 9) for measurements conducted in the northern hemisphere (Girard et al., 2007). No signal is obtained at distances >160 m from the loop center. At a distance of about 120 m from the loop center

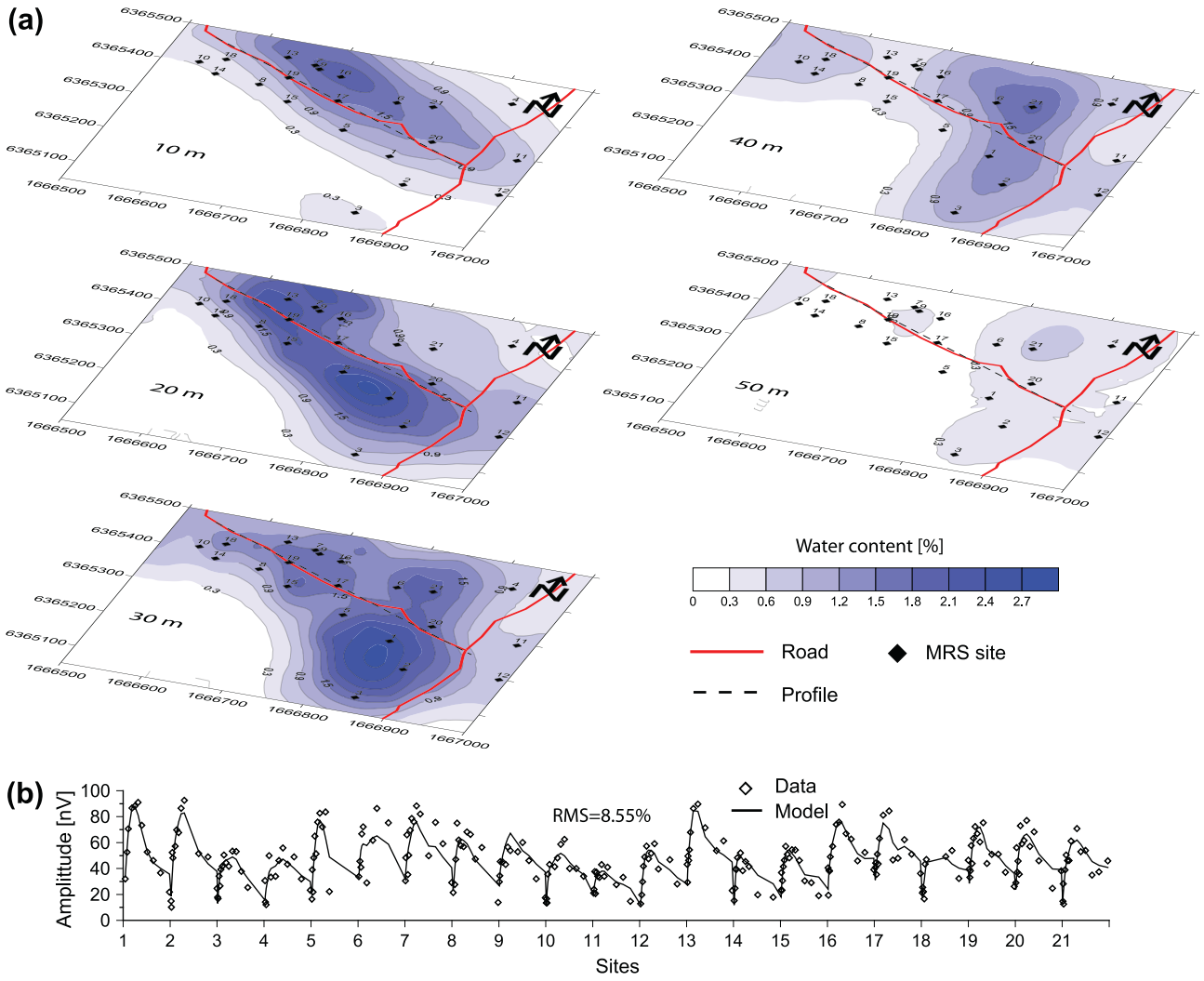

Fig. 10. (a) Water content distribution at different depths from 3D inversion. (b) Inversion fit where measured signals (diamonds) and calculated signals (solid line) are plotted against the normalized pulse moments.

signals of 10–20 nV can be expected, which determines the boundary of the exposed area of one loop.

3.5.4. 3D Inversion and modeling result

The data have been inverted with both amplitude and complex inversion for different regularizations for the cell size $40 * 40 * 5\ m^3$, where the amplitude inversion has been chosen to present the final model. An approximate solution is found through the minimization of the Tikhonov's function (Legchenko et al., 2011). However, the final choice of regularization was determined from comparison of MRS with the RMT resistivity distribution, as RMT clearly distinguish the limestone–marl interface. The inverted voxel model is here presented as depth slices at depths of 10, 20, 30, 40 and 50 m (Fig. 10a). The water content varies between 0% and 3%, where most of the water in the investigated area is distributed along a 200 m wide corridor stretching from the north-west to south-east, corresponding to the major fault direction in the area. The water content maximum is found between 20 and 30 m in depth. There is an indication of two water bodies, one in the north-western and one in the south-eastern corner, respectively. This can best be seen at depths of 20–30 m with two water content maxima. Below 50 m in depth there is hardly any water at all.

A more blocky model has also been tested to fit the data (Fig. 11a–c) by dividing the investigation area into different model blocks (Fig. 11b), where each block differ in size, depth and water content. Here, the vertical and lateral extensions of the blocks have been defined from 3D inversion result (Fig. 10a) and from the maximum amplitude distribution (Fig. 11a). On basis of this, the estimated volume of water is about 100,000 m^3 in both the inverted voxel and blocky models and it can be seen that the blocky model gives a reasonable fit.

The quite homogenous maximum amplitude distribution in the study area together with the similarities between the 1D and 3D inversion models suggest that the 1D inversion gives reliable results. However, in the 3D inverted model, the estimated water content is usually a little bit higher and discontinuities in the groundwater distribution become more obvious.

4. Integrated interpretation

From CR measurements it is possible to estimate the resistivity of the limestone with a varying content of marl. A relatively homogenous limestone has a resistivity of >5000 Ωm and a corresponding porosity of <1%, whereas higher concentrations of marl result in resistivities ⩽2000 Ωm and porosities between 3% and 5%. In one sample, the content of marl seems to exceed the content of limestone and the resistivity is then as low as 140 Ωm with a corresponding porosity of 10%. From resistivities defined with CR,

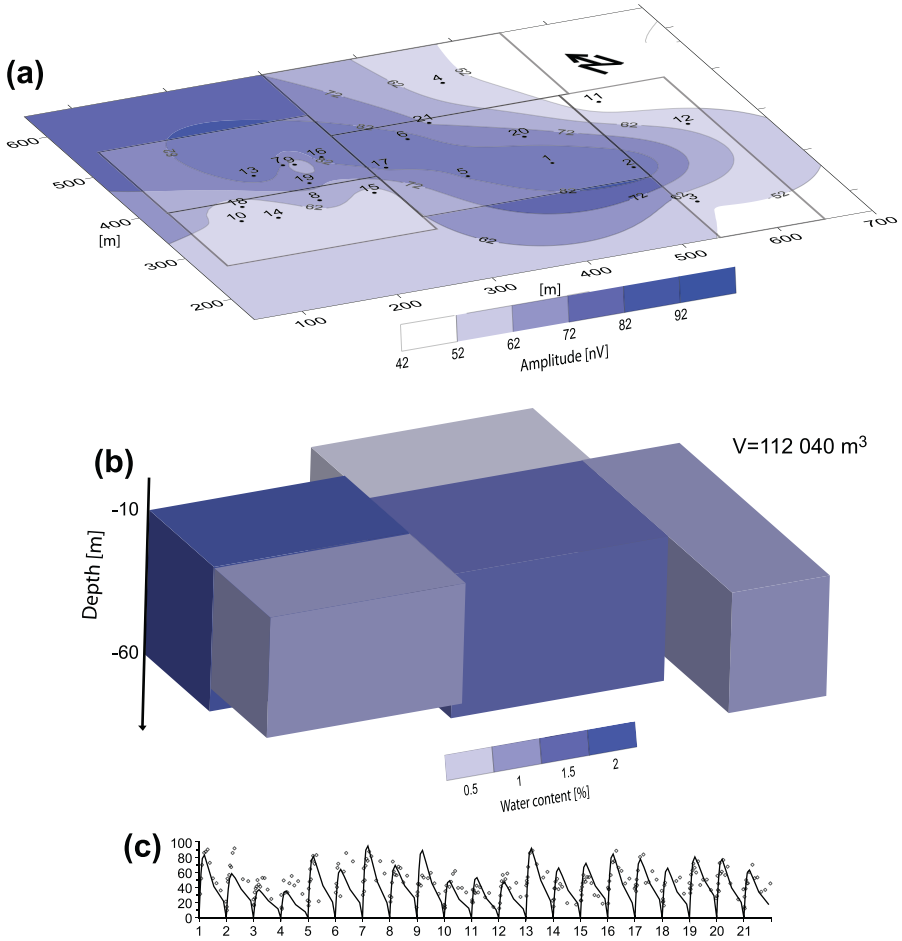

Fig. 11. (a) Sites and boxes plotted above a contour map with maximum amplitudes. (b) Box model. (c) Model fit, where field data (diamonds) and model (solid line) are plotted against the normalized pulse moments.

both the RMT and the VES methods can distinguish the high resistive potentially water bearing limestone from the underlying impermeable marlstone at depths between 40 and 60 m, with marlstone closer to the surface at a distance between 100 and 250 m along the profile (Fig. 12a). The parallel MRS section shows that the water content here varies between 0% and 3% and is distributed from the surface and downward to about 50 m, with little or no water at a distance between the profile coordinates 100 and 250 m (Figs. 10a and 12b) where the marl is closer to the surface. The RMT resistivity is also lower in the limestone in this section, which could suggest a greater concentration of marl as defined by the CR measurements and therefore less measureable water by MRS. This decrease in resistivity could also be the result of a fractured limestone, however no indication of that is seen in the MRS or GPR data. The maximum water content generally coincides with the high resistive limestone at depths of 20–40 m where one instead would expect a decrease in resistivity. In the north-western part of the area (outside the map in Fig. 3) limestone outcrops and GPR clearly distinguish between the upper soil cover and the limestone located at a depth of 0.5 m in the western area, with a maximum of about 4 m in the middle of the profile, (Fig. 12c). Between profile coordinates 250 and 400 m, a second layer appears at a depth of about 3–4 m, which can be seen in VES3 as a low resistive layer (80 Ωm), which could be interpreted as saturated swampy soil or fractured limestone. The top, low resistive layer of the RMT section is clearly thicker in this area as well. RMT indicates a low resistive layer possibly associated with saline water, starting at a depth of 80 m between profile coordinates 150 and 300 m, seen by VES2 and VES3 as well. From the MRS measurements no water can be detected at this depth, which implies that the indicated saline layer is associated with marlstone.

5. Discussion

5.1. Variation of resistivity and porosity

The RMT and CR data show similar range of resistivities, whereas the inverted VES resistivities are generally higher. This could to some extent be explained by the interbedding of marl and limestone. The induced current flow from RMT is mainly horizontal and the current will hence mostly flow through the more conductive marl, whereas the injected current from VES will be conveyed through both the more resistive limestone and the marl, resulting in higher resistivities in the VES model (Seidel, 2005). A combination of the two methods could in this way distinguish highly anisotropic limestone. The smoother multilayer RMT model could also generate lower resistivities compared to the VES block model. The borehole samples from the Ala-1 borehole show that there is a smooth transition from massive limestone to more interbedded limestone-marl, which favors the choice of a smooth resistivity model. Archie's formula (Archie, 1942) for a saturated medium: $\rho_{aq} = \rho_w \cdot \Phi^{-m}$, where ρ_{aq} and ρ_w denotes the aquifer and water resistivity, respectively and Φ the porosity, can be used to roughly estimate the aquifer resistivity for a porous medium. The cementation factor m can vary from about 1 in loosely consolidated rock to about 3 in well indurated limestone (Gluyas and

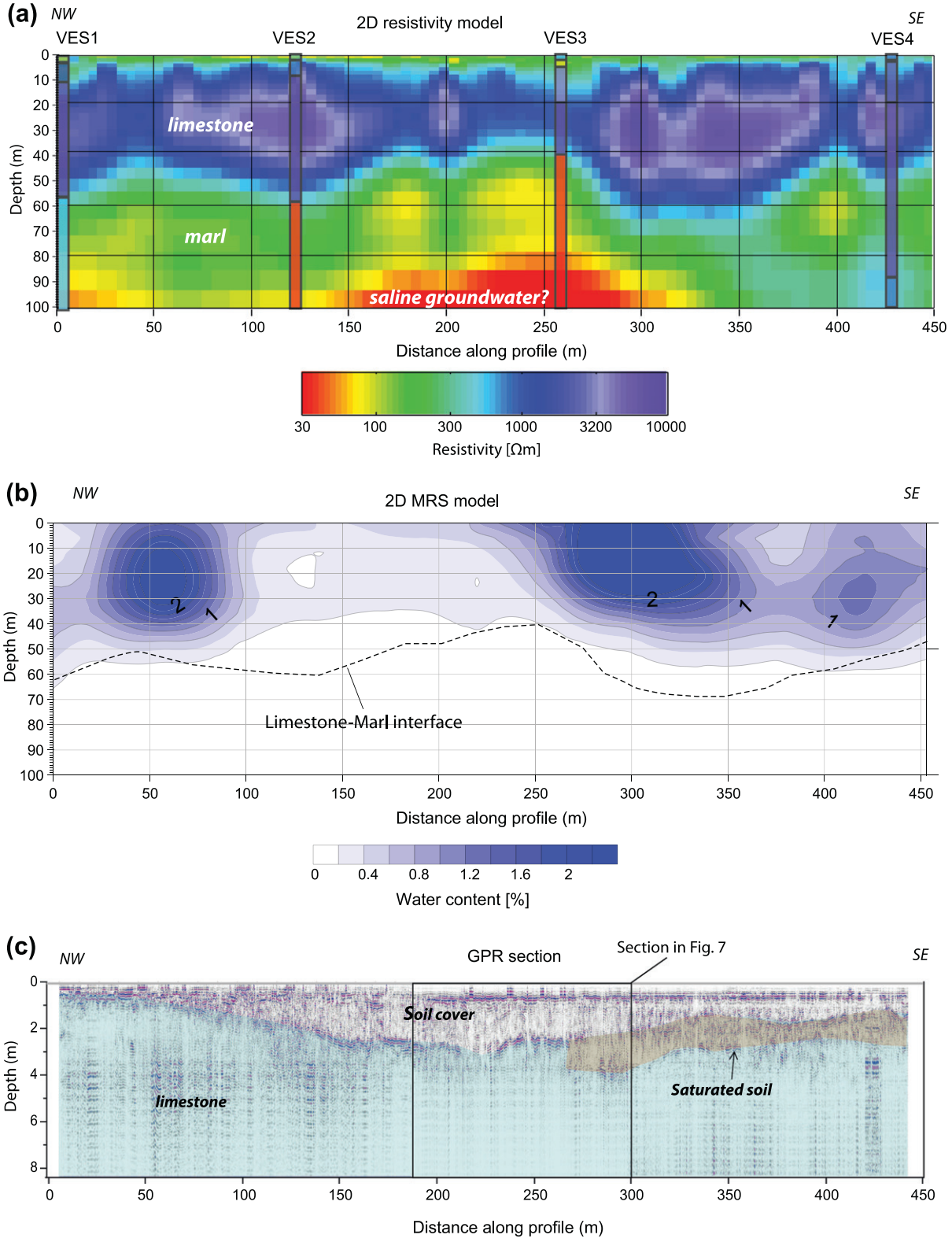

Fig. 12. Cross-section oriented along the trail trending NW-SE (Fig. 3) for (a) Resistivity RMT and VES data (Ωm); (b) MRS water content (%) and (c) GPR radargram (OBS! Note the difference in vertical scale).

Swarbrick, 2004). All the samples from the Ala-1 borehole have an m varying between 1.8 and 2.2 determined from porosity and resistivity measurements. The monitored wells in this area have on average a ρ_w of 20 Ωm (Eklund, 2005). For a porosity varying between 2% and 5%, the ρ_{aq} differ between 5000 and 100,000 Ωm, corresponding quite well to the measured resistivity values in field. Furthermore, the short T_{1MRS} (<400 ms) and T_2^* (≈100–250 ms) relaxation time, strongly suggests that the water is detained by a porous medium rather than larger fractures. Still, the maximum water content amounts to ca. 3% and ca. 2.5% from the 3D and 1D inversion, respectively, which is clearly more than the measured porosities of the homogenous limestone in the borehole

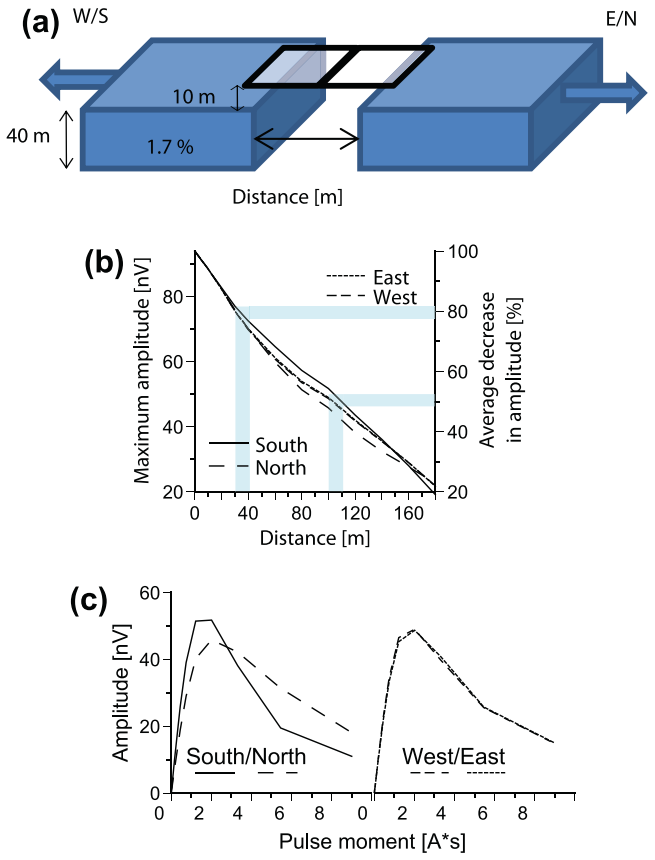

Fig. 13. (a) Modeling of two blocks separated between 0 and 180 m for two side-by-side loops in the North–South and East–West directions. (b) The maximum amplitude decreases gradually to about 20% of the maximum value at a separation of 180 m. (c) The asymmetry in signal distribution between the two loops in South/North direction at a distance of 100 m is due to the inclination of the earth magnetic field (see Fig. 9).

samples (<1%). This suggests that the aquifer is related to a secondary porosity originating in small fractures, molds and vugs, rather than the primary porosity of the limestone or larger fissures and cavities.

5.2. Connectivity of aquifers

MRS cannot determine the direction of flow. However, MRS can detect natural barriers separating water bodies from each other. Legchenko et al. (2011) illustrates how to minimize the number of loops, while keeping acceptable accuracy and resolution. They show that half-side overlap loops are the best compromise, while side-by-side loops, although the lower accuracy, still can give reasonable results. The two water content maxima in the north-western and south-eastern parts could be an indication of two different aquifers (Fig. 12b), separated by limestone with a higher degree of marl. Modeling of two blocks (with water content and aquifer geometry corresponding to the investigated area) separated horizontally by 0–180 m illustrates, that at about 35 m the amplitude has decreased by 20%, which, considering the local noise conditions, probably is the best resolution possible for this loop configuration. At about 100 m separation, the amplitude decreases to about half and at about 180 m only 20% of the signal is left. This kind of barrier could be more easily identified in the north–south than east–west direction, due to the asymmetry of the signal amplitude distribution between the two loops (Figs. 13c and 9). However, the results also suggest the necessity of using both MRS and RMT to be able to locate these kinds of barriers.

6. Conclusions

In this study the geophysical methods MRS, RMT, VES and GPR were tested for characterizing aquifers in Gotland, in respect to geometry and storage as well as the connectivity of the aquifer over a more extensive area. The use of multiple techniques has shown to give a more coherent interpretation but also a more complete picture of the groundwater situation in the area. However, the shallow penetration depth of GPR and the lack of soil cover in some places of the investigated area make geoelectrical methods and GPR less efficient.

MRS identifies the aquifer at depths between 10 and 60 m with maximum water contents at depths of 20–30 m. The water content varies between 0% and 3% and the decay time (T_{1MRS}) is less than 400 ms suggesting that the aquifer medium consist of small fractures, molds and vugs rather than larger karst fractures and cavities. The boundaries between overburden, limestone and marl can be identified by RMT and VES. The peak water content measured with MRS usually coincides with the most resistive sections of the limestone, but no clear correlation can be seen between water content and resistivity. MRS is therefore the only method in this survey that actually detects water and thus determines the vertical and lateral distribution of water within the aquifer together with the free volume of water.

Two potential aquifers were identified with MRS, possibly separated by marlstone. From modeling of two water saturated blocks it can be seen that a boundary between such two separated aquifer can be more easily discriminated in N/S-, than E/W direction due to the asymmetry of the signal distribution. RMT has shown to effectively characterize the limestone/marl interface but also to locate anomalous low resistive zones, possibly associated with saline water. RMT also helps to constrain the final MRS model by choosing a suitable regularization for the MRS 3D inversion. All together, the combination of MRS and RMT of the tested methods here seems most efficient and promising for future groundwater explorations in geological environments like in eastern Gotland.

Acknowledgements

This study was funded by the foundation for technological and scientific research in memory of J. Gust. Richert (SWECO). Our deepest appreciation goes to Anatoly Legchenko (Institut de recherche pour le développement) for guidance of MRS 3D inversion and valuable advice in the interpretation of the MRS result. The authors acknowledge the Geological Survey of Sweden (SGU) for providing geological, geophysical and groundwater data from Gotland.

References

Al-fares, W., Bakalowicz, M., Guerin, R., Dukhan, M., 2002. Analysis of the karst aquifer structure of the Lamalou area (Herault, France) with ground penetrating radar. J. Appl. Geophys. 51 (2–4), 97–106.

Anchuela, O.P., Casas-Sainz, A.M., Soriano, M.A., Pocovi-Juan, A., 2009. Mapping subsurface karst features with GPR: results and limitations. Environm. Geol. 58 (2), 391–399.

Archie, G.E., 1942. The electrical resistivity log as an aid in determining some reservoir characteristics. Metall. Petrol. Eng. 146, 54–62.

Bastani, M., 2001. EnviroMT – A New Controlled Source/Radio Magnetotelluric System Ph.D. Acta Universitatis Upsaliensis, Uppsala Dissertations from the Faculty of Science and Technology 32.

Börner, F.D., 1996. Evaluation of transport and storage properties in the soil and groundwater zone from induced polarization measurements. Geophys. Prospect. 44 (4), 583.

Boucher, M., Girard, J.F., Legchenko, A., Baltassat, J.M., Dorfliger, N., Chalikakis, K., 2006. Using 2D inversion of magnetic resonance soundings to locate a water-filled karst conduit. J. Hydrol. 330 (3–4), 413–421.

Daniels, D.J., 2004. Ground Penetrating Radar. Knoval (Institution of Engineering and Technology), London, 734 pp.

Eklund, F., 2005. Förändringar i grundvattenkvaliteten i 19 vattentäkter på Gotland under åren 1989–2004. Länsstyrelsen i Gotlands län, Visby, 133 pp.

Erlström, M., Persson, L., Sivhed, U., Wickström, L., 2009. Beskrivning till regional berggrundskarta över Gotlands län. 978-91-7158-957-6, Sveriges geologiska undersökning, K221.

Girard, J.F., Boucher, M., Legchenko, A., Baltassat, J.M., 2007. 2D magnetic resonance tomography applied to karstic conduit imaging. J. Appl. Geophys. 63 (3–4), 103–116.

Gluyas, J., Swarbrick, R.E., 2004. Petroleum Geoscience. Blackwell Publishing Company, Oxford, UK, 361 pp..

Guerin, R., Benderitter, Y., 1995. Shallow karst exploration using Mt-Vlf and Dc resistivity methods. Geophys. Prospect. 43 (5), 635–653.

Hertrich, M., 2008. Imaging of groundwater with nuclear magnetic resonance. Prog. Nucl. Magn. Reson. Spectrosc. 53 (4), 227–248.

Ismail, N., Schwarz, G., Pedersen, L.B., 2011. Investigation of groundwater resources using controlled-source radio magnetotellurics (CSRMT) in glacial deposits in Heby, Sweden. J. Appl. Geophys. 73 (1), 74–83.

Kalscheuer, T., Pedersen, L.B., Siripunvaraporn, W., 2008. Radiomagnetotelluric two-dimensional forward and inverse modelling accounting for displacement currents. Geophys. J. Int. 175 (2), 486–514.

Legchenko, A., Valla, P., 1998. Processing of surface proton magnetic resonance signals using non-linear fitting. J. Appl. Geophys. 39 (2), 77–83.

Legchenko, A., Valla, P., 2002. A review of the basic principles for proton magnetic resonance sounding measurements. J. Appl. Geophys. 50 (1–2), 3–19.

Legchenko, A., Baltassat, J.M., Bobachev, A., Martin, C., Robain, H., Vouillamoz, J.M., 2004. Magnetic resonance sounding applied to aquifer characterization. Ground Water 42 (3), 363–373.

Legchenko, A., Ezersky, M., Camerlynck, C., Al-Zoubi, A., Chalikakis, K., Girard, J.F., 2008. Locating water-filled karst caverns and estimating their volume using magnetic resonance soundings. Geophysics 73 (5), G51–G61.

Legchenko, A., Descloitres, M., Vincent, C., Guyard, H., Garambois, S., Chalikakis, K., Ezersky, M., 2011. Three-dimensional magnetic resonance imaging for groundwater. New J. Phys. 13, 1–17.

Linde, N., Pedersen, L.B., 2004. Evidence of electrical anisotropy in limestone formations using the RMT technique. Geophysics 69 (4), 909–916.

Lindewald, H., 1985. Salt grundvatten i Sverige, rapporter och meddelanden. 39. Sveriges geologiska undersökning, Uppsala.

Lubczynski, M., Roy, J., 2003. Hydrogeological interpretation and potential of the new magnetic resonance sounding (MRS) method. J. Hydrol. 283 (1–4), 19–40.

Olofsson, B., 1996. Salt groundwater in Sweden – occurence and Origin, Rapporter och meddelanden nr 87. In: IM, S.W. (Ed.), 14th Salt Water Intrusion Meeting. Geological Survey of Sweden, Malmö, Sweden, pp. 91–100.

Pedersen, L.B., Engels, M., 2005. Routine 2D inversion of magnetotelluric data using the determinant of the impedance tensor. Geophysics 70 (2), G33–G41.

Pedersen, L.B., Bastani, M., Dynesius, L., 2005. Groundwater exploration using combined control led-source and radiomagnetotelluric techniques. Geophysics 70 (1), G8–G15.

Pelton, W.H., Ward, S.H., Hallof, P.G., Sill, W.R., Nelson, P.H., 1978. Mineral discrimination and removal of inductive coupling with multifrequency-IP. Geophysics 43 (3), 588–609.

Persson, L., Erlström, M., Bastani, M., Pedersen, L.B., 2008. Airborne VLF measurement over the island of Gotland, Sweden, Extended abstract AEM2008. In: 5th International Conference on Airborne Electromagnetics, Haikko Manor, Finland, pp. 28–30. .

Seidel, K., 2005. Elektromagnetische Zweispulen-Systeme, Prinzip der Methode. In: Knödel, K.K.K., Lange, G. (Eds.), Handbuch zur Erkundung des Untergrundes von Deponien und Altlasten. Springer, Berlin Heidelberg, NewYork.

SEPA, 2007. Environmental Quality Criteria for Groundwater, Swedish Environmental Protection Agency (SEPA).

Shirov, M., Legchenko, A., Creer, G., 1991. A new direct non-invasive groundwater detection technology for Australia. Explor. Geophys. 22, 333–338.

Siripunvaraporn, W., Egbert, G., 2000. An efficient data-subspace inversion method 2-D magnetotelluric data. Geophysics 65 (3), 791–803.

Triumf, C.-A., Thunehed, H., Antal, I., 2000. Bestämning av elektriska egenskaper hos vulkaniter från Skellefte- och Arvidsjaurgrupperna. Sveriges geologiska undersökning 2000:8: 30 pp.

Turberg, P., Müller, I., Flury, F., 1994. Hydrogeological investigation of porous environments by radio magnetotelluric-resistivity (RMT-R 12-240 kHz). J. Appl. Geophys. 31 (1–4), 133.

Vattenmyndigheten, 2007. Miljöövervakning av vatten – tillstånd hos inlands-. kust- och grundvatten i Södra Östersjöns vattendistrikt, Kalmar, 186 pp.

Vouillamoz, J.M., Legchenko, A., Albouy, Y., Bakalowicz, M., Baltassat, J.M., Al-Fares, W., 2003. Localization of saturated karst aquifer with magnetic resonance sounding and resistivity imagery. Ground Water 41 (5), 578–586.

Worthington, P., Collar, F.A., 1982. The relevance of induced polarization to quantitative formation evaluation. In: Transactions of the SPWLA Annual Logging Symposium, 23.